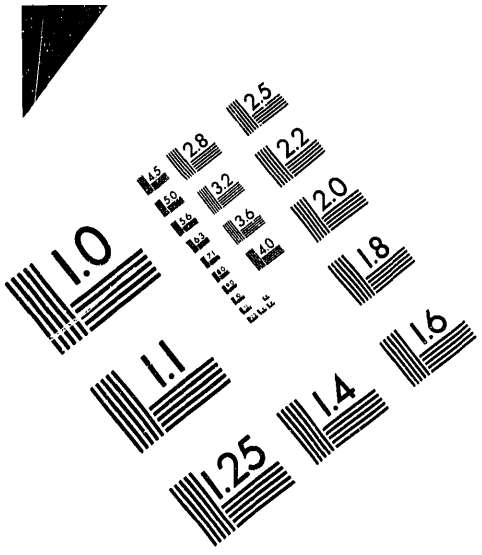

Association for Information and Image Management

1100 Wayne Avenue, Suite 1100
Silver Spring, Maryland 20910

301/587-8202

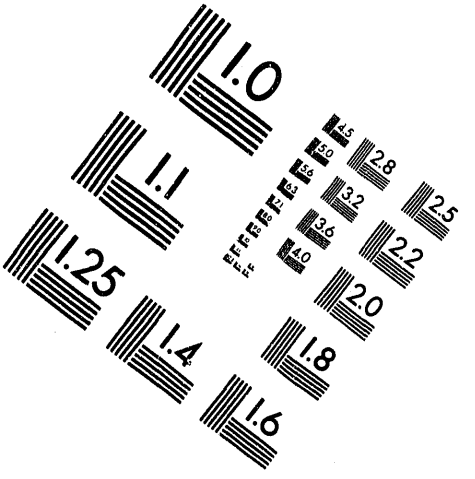

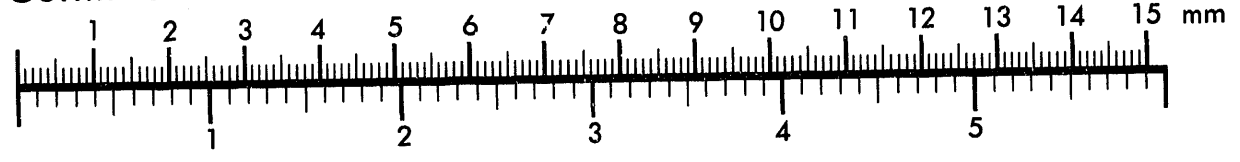

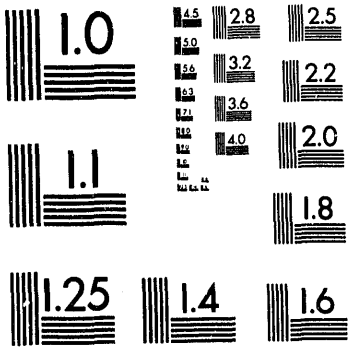

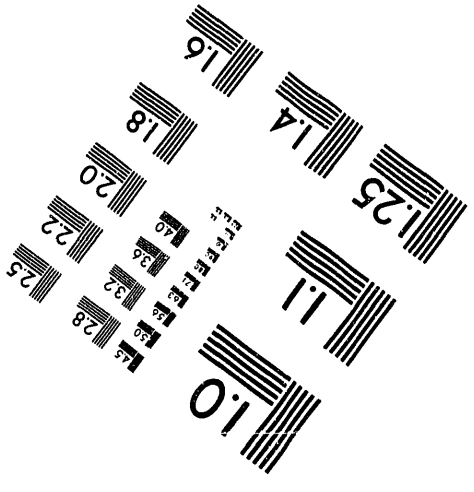

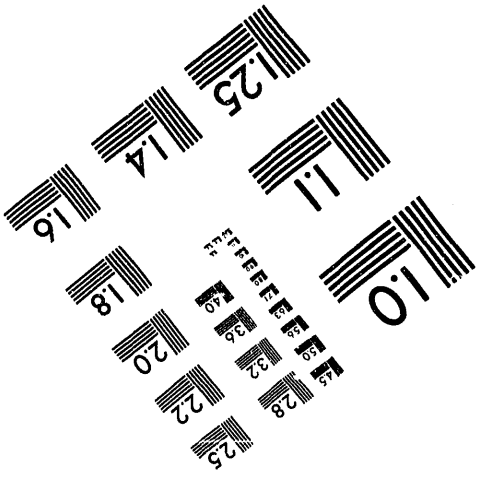

MANUFACTURED TO AIIM STANDARDS
BY APPLIED IMAGE, INC.

1 of 1

LBL-33447

Flow Visualization and Relative Permeability Measurements in Rough-Walled Fractures

Peter Persoff and Karsten Pruess

Earth Sciences Division
Lawrence Berkeley Laboratory
University of California
Berkeley, California 94720

January 1993

This work was supported, through U.S. Department of Energy Contract No. DE-AC03-76SF00098, by the Director, Office of Civilian Radioactive Waste Management, Office of External Relations, administered by the Nevada Operations Office in cooperation with the Swiss National Cooperative for the Disposal of Radioactive Waste, and by the Assistant Secretary for Conservation and Renewable Energy, Geothermal Division.

Presented at Fourth International High-Level Radioactive Waste Management Conference, Las Vegas, NV April 26-30, 1993.

FLOW VISUALIZATION AND RELATIVE PERMEABILITY MEASUREMENTS IN ROUGH-WALLED FRACTURES

P. Persoff and K. Pruess
Lawrence Berkeley Laboratory
Earth Sciences Division*
Berkeley, California 94720
(510) 486-5931

ABSTRACT

Two-phase (gas-liquid) flow experiments were done in a natural rock fracture and transparent replicas of natural fractures. Liquid was injected at constant volume flow rate, and gas was injected at either constant mass flow rate or constant pressure. When gas was injected at constant mass flow rate, the gas inlet pressure, and inlet and outlet capillary pressures, generally did not reach steady state but cycled irregularly. Flow visualization showed that this cycling was due to repeated blocking and unblocking of gas flow paths by liquid.

Relative permeabilities calculated from flow rate and pressure data show that the sum of the relative permeabilities of the two phases is much less than 1, indicating that each phase interferes strongly with the flow of the other. Comparison of the relative permeability curves with typical curves for porous media (Corey curves) show that the phase interference is stronger in fractures than in typical porous media.

INTRODUCTION

Two-phase flow conditions are likely to exist in the rock formations surrounding high level nuclear waste repositories, either because the repository itself is located above the water table (e.g. Yucca Mountain), because gas may be present naturally below the water table (e.g. Oberbauenstock and Wellenberg in Switzerland, possibly also at WIPP), or because gas may be released below the water table by corrosion, bacterial action or radiolysis.[1] In fractured media, the fractures generally conduct much more flow than the matrix. With proposed repositories situated in fractured crystalline rock (e.g., Oberbauenstock, Wellenberg) or fractured tuff (e.g. Yucca Mountain), understanding and quantifying gas-liquid flow in fractures is important for mathematical and numerical simulation of waste repositories. Two-phase flow in fractures also arises in the exploitation of geothermal and petroleum reservoirs, and extraction of coal-bed methane.

For modeling unsaturated flow, either in porous media or in fractures, relative permeability functions quantify the degree to which each phase impedes the flow of the other. The relative permeability is defined by

$$k_i = k k_{r,i}$$

where k_i is the effective permeability to phase i, k is the intrinsic permeability of the medium, and $k_{r,i}$ is the relative permeability to phase i. When the medium is completely saturated with phase i, $k_{r,i} = 1$. In porous media, the $k_{r,i}$ are generally strong and nonlinear functions of phase saturation. This makes relative permeability functions critical to mathematical modeling of flow in unsaturated porous media.

A goal of the present work is to observe two-phase flow behavior and measure relative permeabilities in fractures, and to compare them with relationships measured for three-

This work was supported in part by the Director, Office of Civilian Radioactive Waste Management, Office of External Relations, administered by the Nevada Operations Office in cooperation with the Swiss National Cooperative for Disposal of Radioactive Waste (Nagra), and in part by the Assistant Secretary for Conservation and Renewable Energy, Geothermal Division, of the U.S. Department of Energy, under contract no. DE-AC03-76SF00098.

dimensional porous media, and theoretical predictions based on fracture geometry. While the cubic law for single-phase flow in fractures has been well established theoretically and experimentally, measurements of two-phase flow remain scarce, and results have been contradictory. Generally, modelers have taken $k_{r,i} = S_i$, where S is saturation. This leads to $k_{r,w} + k_{r,nw} = 1$, where subscripts w and nw refer to wetting and nonwetting phases respectively.[2] Physically, this can be interpreted as meaning that each phase flows in its own flow paths and does not interfere with the other. This model seems to be based upon early experimental work[3] and analysis of field data from geothermal fields (steam and water).[4] Recent theoretical work and numerical simulations[2,5] of two-phase flow in fractures with variable aperture (i.e., rough-walled fractures) have shown strong phase interference, with $k_{r,w} + k_{r,nw}$ much less than 1.

In this paper we report flow-rate and pressure-drop measurements from three experiments, using both natural rock fractures and transparent replicas of natural fractures. The use of transparent replicas allows direct observation of the distribution of phases in the fracture. In all cases the two fluid phases used were nitrogen gas and water. The experimental setup is shown in Figure 1, and conditions are summarized in Table 1. In all experiments liquid was injected at controlled volume flow rate. Gas was injected at either controlled mass flow rate or controlled pressure. The data show that when gas was injected at constant mass flow rate, pressure drop was often non-steady and cycling. We explain this behavior, on the basis of videotaped observations, as resulting from repeated blocking and unblocking of gas flow paths. To avoid such pressure cycling, gas was injected at controlled pressure. Finally, we present curves for relative permeability calculated from flow rates and pressure drops.

EXPERIMENT

Only a brief summary of methods and materials is presented here; a detailed description is available elsewhere.[6,7] Measurements were made in both a natural rock fracture and in transparent replicas of natural fractures. The fracture for experiments A through C was found in a granite core from the Stripa mine in Sweden, which has been used as a natural underground laboratory for the study of hydrologic issues related to high level waste management since 1976. The prototype fracture for Experiment D was a natural fracture in tuff from the Dixie Valley, NV geothermal area.[8] Transparent replicas of the fractures were prepared by making silicone rubber molds of each face of the fracture, and then pouring Eccobond 27 epoxy in the molds. The apertures of the transparent replicas were measured by light attenuation. Two digitized images of the fracture replica, once filled with water, and once with dye, were compared pointwise. The aperture was then calculated from the ratio of light intensity in the two images, using Beer's law. A 3-dimensional plot of aperture over x-y space can be considered as a rough surface; the fractal dimensions of these surfaces have been estimated.[9] The Dixie Valley fracture shows obvious anisotropy; in Experiment D flow was in the direction of greatest permeability.

The Stripa fracture was approximately perpendicular to the axis of a 115-mm diameter core; this allowed sandwich-like rectangular specimens to be machined from both the core and the replica, 20.7 mm thick, 74.9 mm wide, and 81.3 mm long. Special endcaps were then fabricated to match the width of the sample.

The apparatus was designed to measure the inlet and outlet pressures of two immiscible fluids as they flow through a fracture (see Figure 1). Special endcaps, modified from the design of Hassler,[10] were fabricated to inject and receive two immiscible fluids at different pressures, so that controlled capillary pressure boundary conditions are imposed at the inlet and outlet. The wetting phase (water in these experiments, with biocide added to prevent bacterial growth which would clog the fracture) is injected to the inlet edge of the fracture through a wettable porous ceramic block, with 1 bar air-entry pressure. The nonwetting phase (nitrogen gas in these experiments) is injected directly to the fracture edge through a plenum and grooves in the porous block.

Four pressure taps sensed the inlet and outlet gas pressure, and inlet and outlet liquid pressures. Four absolute pressure transducers were connected to the taps, and four differential pressure transducers were connected across pairs of taps to measure the pressure drop in the gas phase, pressure drop in the liquid phase, inlet capillary pressure, and outlet capillary pressure. These redundant measurements provided greater precision than subtracting the readings of the absolute pressure transducers, and also provided a check of the data. During experiments, the

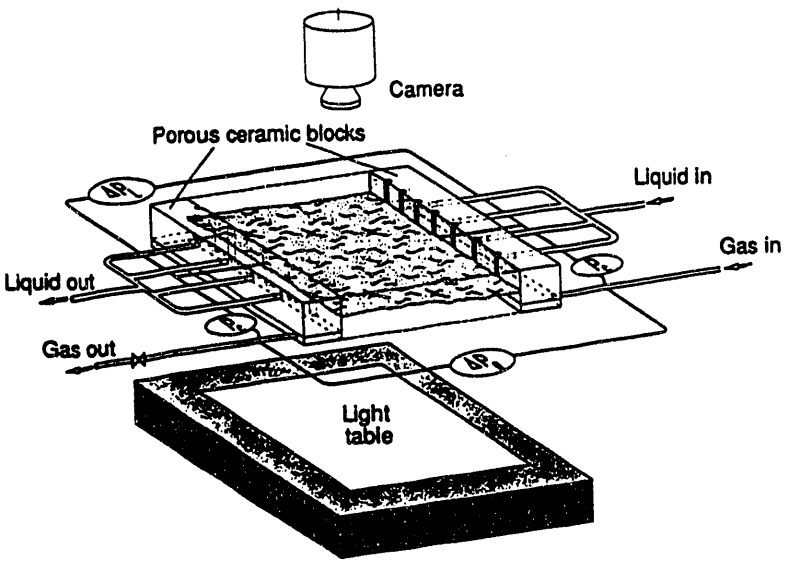

Figure 1. Apparatus for flow visualization and relative permeability measurement in transparent replica of a natural rock fracture. Ovals represent differential pressure transducers; absolute pressure transducers have been omitted for clarity. Note that gas is injected to a plenum which distributes it to vertical grooves in the porous block at the inlet end. Only seven grooves are shown in the figure; actually they are closely spaced with a total of 40 grooves. Rubber-lined steel bars which seal edges are not shown.

Table 1. Two-phase flow experiments in Rough-Walled Fractures.

Exp.	Fracture	Gas injection	Liquid injection	Comment
A	Stripa, replica 1	constant mass rate	constant volume rate	results in ref. (6)
B	Stripa, replica 2	constant mass rate	constant volume rate	videotape observations of liquid slug motion, see Fig. 3
C	Stripa, natural rock	constant mass rate	constant volume rate	Data in Table 2 and Figs 2, 5, 7
D	Dixie Valley replica	constant pressure	constant volume rate	Data in Table 3 and Figs 4, 6-8

inlet capillary pressure was observed and the outlet capillary pressure was controlled to match the inlet capillary pressure (time-averaged if the inlet capillary pressure was not steady). In experiments A through C outlet capillary pressure was adjusted by allowing liquid to exit to barometric pressure, and adjusting the gas outlet pressure by choking the gas exit flow through a needle valve. In Experiment D it was done by allowing gas to exit to barometric pressure, and draining the liquid outflow through a completely filled flexible tube with its outlet submerged in a liquid-filled beaker; the beaker was located below the plane of the fracture and its liquid surface elevation was adjusted to control the liquid outlet pressure.

Note in Figure 1 that the location of the liquid tap allows measurement just at the edge of the fracture, downstream of the inlet porous block and upstream of the outlet porous block. A 1-mm thick plug of porous ceramic was placed in the tip of the liquid pressure taps to prevent gas from invading them. The gas pressure taps were placed in the inlet and outlet lines; separate measurements were done to confirm that the pressure drop between this point and the gas plenum was negligible, at these flow rates. Liquid was injected by an ISCO syringe pump, and gas was injected through a Brooks mass-flow controller or directly from a two-stage regulator.

PROCEDURE

The apparatus was assembled, and the permeability to gas was measured. Then it was evacuated and saturated with liquid, and the permeability to liquid was measured. The procedure for experiments A through C was as follows: with liquid flowing, gas injection was started to establish the first two-phase flow condition. At intervals, the fractional flow of gas was increased, by alternately increasing the gas flow rate or decreasing the liquid flow rate. In this manner a total of 13 two-phase flow conditions were studied, with increasing gas-liquid flow rate ratio, and with pressure drop across the fracture generally constant. Pressure measurements were made for each condition. In general, the pressure measurements showed that no steady state developed, but instead the pressures cycled more or less irregularly around average values. As a result, the outlet capillary pressure could not be matched to the inlet capillary pressure, except as an average. For condition 1, with the highest liquid flow rate, the liquid outflow rate was measured by timing drops leaving the apparatus. The gas and liquid flow rates during each of the flow conditions for Experiment C are summarized in Table 2.

Table 2. Flow rates and permeabilities in experiment C.

Q_g (cm^3/min)	Q_L (mL/hr)	Mass Flow Ratio	k_{rL}	k_{rg}
0.520	15.00	0.00259	0.2257	0.00781
0.520	8.00	0.00487	0.1468	0.00995
1.020	8.00	0.00955	0.1264	0.01665
1.020	4.00	0.01911	0.07473	0.02027
2.020	4.00	0.03785	0.07160	0.03746
2.020	2.00	0.07570	0.03847	0.04200
4.030	1.00	0.3021	0.01961	0.08311
8.030	1.00	0.6019	0.01463	0.1144
8.030	0.50	1.204	0.008580	0.1420
17.249	0.50	2.586	0.009455	0.3495
24.126	0.36	5.023	0.006944	0.4964
18.628	0.18	7.757	0.004844	0.5343
27.890	0.09	23.23	0.002275	0.7356

For Experiment D, the procedure was different: While the fracture was saturated with liquid, a dye tracer test was done. Then, with liquid flowing at a constant rate, gas injection pressure was applied (i.e., inlet capillary pressure > 0). Gas invaded and partly desaturated the fracture, but for several step increases of gas pressure, no complete gas flow path to the outlet was established. Instead, the gas flow was blocked when the capillary pressure at the forward tip of the gas finger was insufficient to invade any further. The pressure drop across the fracture increased, indicating that the partial invasion of gas had reduced the liquid relative permeability while the gas relative permeability was still zero. Eventually gas broke through to the outlet and a complete gas flow path was established. A series of measurements was made in which gas was injected at constant pressure and liquid at stepwise decreasing volume flow rates. When gas was injected at constant pressure, its flow rate was monitored by occasionally diverting it through a reversible flow loop of transparent nylon tubing in which the motion of a liquid slug could be timed. The data for Experiment D are shown in Table 3.

RESULTS

In this section we first direct attention to the non-steady behavior during several of the two-phase flow conditions in Experiment C. The flow visualization observations made in Experiments A and B are introduced to explain this behavior, and the time-averaged data for each of the two-phase flow conditions are used to calculate relative permeability curves.

Next the data from Experiment D are presented. With increasing inlet capillary pressure, the liquid relative permeability decreases, while gas relative permeability is still zero, until the first gas flow path is established. Then as liquid flow rate decreases, inlet capillary pressure increases, while the fracture desaturates with decreasing liquid relative permeability and increasing gas relative permeability.

EXPERIMENT C

Pressure and flow rate data for Experiment C, averaged for each two-phase flow condition, are summarized in Table 2. Generally, the outlet liquid pressure was steady, but the outlet gas pressure and both inlet pressures cycled irregularly. As an example, pressures measured during the fourth two-phase flow condition are shown in Figure 2. Generally, the pressures cycled irregularly around average values, but at times the pressure cycling stopped; and at others, it became very regular. As the gas:liquid ratio increased, the size of the pressure excursions decreased relative to the pressure drop across the fracture, as did their frequency. When the gas:liquid mass flow rate ratio was greater than 1, such pressure excursions were essentially eliminated.

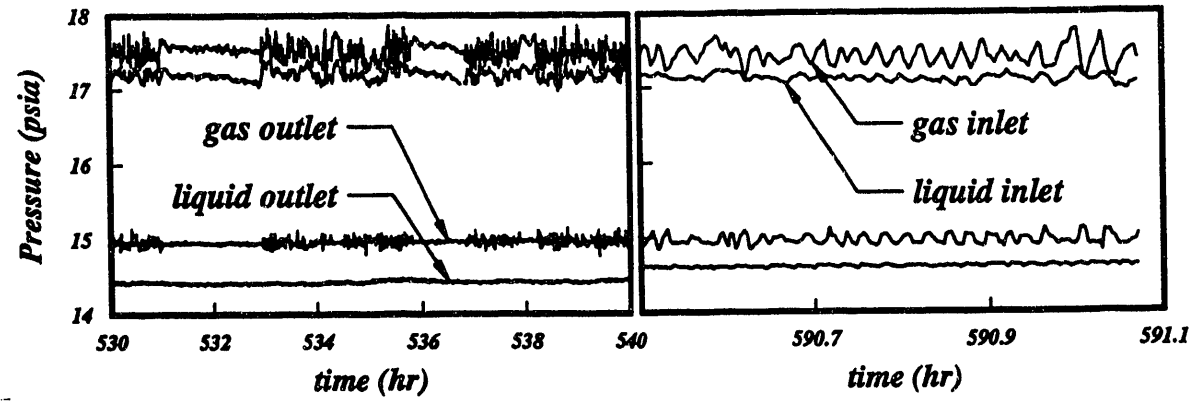

Figure 2. Absolute pressures measured during Experiment C, fourth condition. Note scale break. Stability from 531 to 533 hours and 536 to 537 hours suggests that phase occupancy was delicately balanced until disturbed by vibrations, while regular cycling of inlet and outlet gas pressures between 590.7 and 590.9 hours suggests that one gas flow path was repeatedly blocked and unblocked at the same critical pore.

To further examine the failure of the system to come to steady state, we reviewed videotapes from Experiment B. A videotape record was available for the period shown in Figure 3. Because water matches the refractive index of the cured epoxy more closely than gas, water-occupied portions of the fracture replica appear brighter than gas-occupied portions. When viewing the videotape, no motion can be seen when gas and liquid are flowing in their own flow paths. Motion can only be seen when some portion of the fracture changes from gas-occupied to liquid-occupied or the reverse. Such phase-occupancy-change events (POC events) appeared to occur instantly and generally lasted only a few seconds. Typically, a slug of water would emerge from the liquid-occupied area and invade a gas flow path, move quickly along the gas flow path for one or two centimeters, and then disappear back into the liquid-occupied area. Afterward, there would often be a slight change in the overall pattern of phase occupancy in the fracture replica. By tracing the location of such motion on the monitor, it became clear that all such events occurred along two paths through the fracture; comparison with the aperture map showed that, as expected, they were in the regions of greatest aperture. Often, an event along one part of the flow path would be followed within a minute or so by an event further along the same path. The occurrence of POC events are noted in Figure 3. POC events along the "lower" flow path were associated with maxima in gas inlet pressure and inlet capillary pressure; this indicates unblocking of a gas flow path. However they probably are not the cause of the unblocking, because such events were also

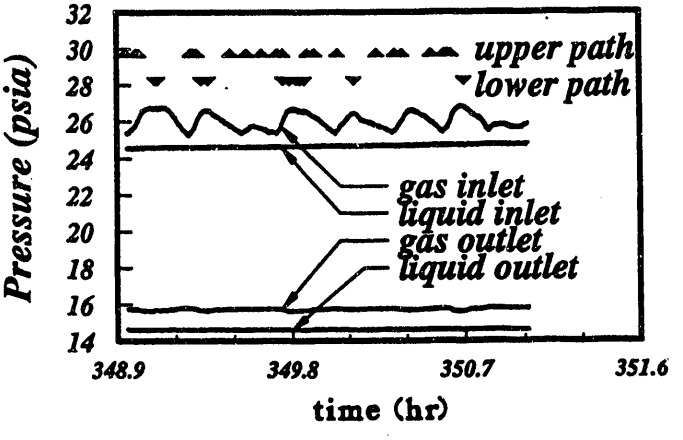

Figure 3. Absolute pressures measured during Experiment B. Tick marks show times when phase-occupancy-change events were observed. All such events occurred along two flow paths.

observed in Experiment D when the gas flow path was continuously open.

EXPERIMENT D

The dye tracer experiment showed the most permeable liquid flow paths, first as threads of color, then widening and darkening as more dye accumulated in the flow paths. The pressures measured during gas invasion are shown in Figure 4. As gas injection pressure was increased stepwise, gas fingers penetrated into, but not completely through the fracture. With these stepwise decreases of liquid saturation, the pressure drop in the liquid phase increased, indicating reduced liquid permeability. The first

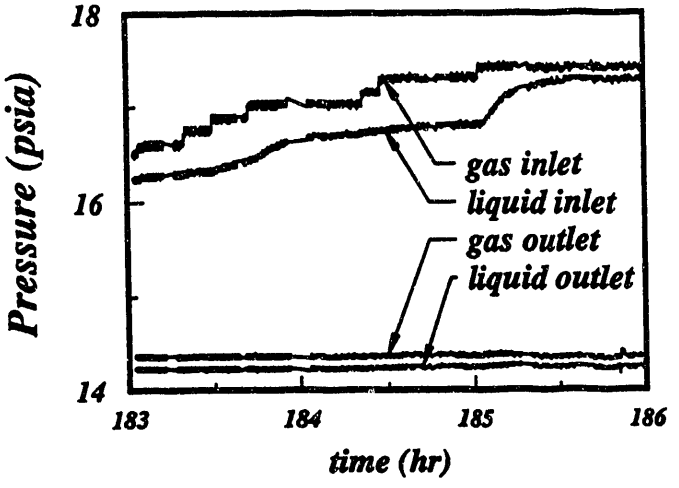

Figure 4. Absolute pressures measured during initial invasion of gas into liquid-filled fracture, Experiment D. The gas inlet pressure was increased stepwise, but not every increase caused additional gas invasion. Liquid flow rate was constant. The pressure drop in the liquid phase, and the liquid inlet pressure, only increased when additional gas invaded, reducing the liquid relative permeability.

gas flow path through the fracture was not the same as the most permeable liquid flow path. Note in Figure 4 that the inlet capillary pressure (difference between gas inlet and liquid inlet pressures) decreased when the first complete gas flow path was established, at 185.1 hours.

Visual observation of the fracture during two phase flow showed that moving liquid slugs were still visible although gas flow paths were not blocked; in fact, this seemed to be an important mechanism of liquid short-cutting across gas-filled large-aperture regions ("lakes") that would be a long way around.. Liquid would accumulate in a bank along the upstream side of the lake, and then jump across to the downstream side. Other times, liquid slugs would move along lakes, apparently propelled by gas behind them. At lower liquid flow rates, such events became less and less frequent. At lower flow rates, too, the liquid slugs pushed by gas became thinner and appeared to be like lamellae moving in foam flow.

DISCUSSION

Cause of pressure cycling in Experiments B and C.

The comparison of visual observations and pressure data indicate that under certain experimental conditions, gas flow paths do not remain continuously open but are continually blocked by liquid. The reason for such continual blocking may be explained as follows: In experiments B and C gas was injected at constant mass flow rate into a liquid-saturated fracture in which liquid is already flowing. When gas is first injected, the capillary pressure increases as gas invades and occupies regions of smaller and smaller aperture in a connected path which does not yet reach to the outlet of the fracture. Eventually gas reaches the outlet along a connected path; the point of minimum aperture along this path will be called the critical pore. When gas first reached this critical pore, its pressure at the pore was determined by pore size and surface tension according to the Young-Laplace law; and its injection pressure was determined by the gas pressure at the critical pore and the additional pressure drop along the path from the inlet to the critical pore. The inlet gas pressure was sufficient to invade this pore, because gas was injected at constant rate. The gas injection pressure was a maximum at the time when the critical pore was invaded. But once the gas flow path has been established, the gas pressure at the critical pore is no longer determined by the Young-Laplace law, but rather by the resistance of the completed flow path and the applied flow rate. The capillary pressure at the critical pore may now be insufficient to keep the pore open, and liquid will reinvade it, at a rate determined by the local pore geometry and the ability of the fracture to deliver liquid to the site. When the pore is liquid-occupied, gas pressure upstream of the pore increases again because the gas flow path network has been partially blocked (or, in the case of a single gas flow path, completely blocked). The gas pressure upstream of the pore increases until the capillary pressure is sufficient for gas to reinvade the pore, and the cycle repeats itself.

According to this discussion, for a system constrained by gas and liquid flow rates, the actual pressures and flow rates through the fracture will tend cycle above and below the points of stable flow, where phase occupancies, pressures, and rates would be constant. The extent of over- and undershoot will depend on fracture geometry, but also on the compressibility and transmissivity of the inlet and outlet plumbing systems. The transient response of the fracture depends on the number of available flow channels, their topology, and their pore-size and permeability distribution. There is a scale effect here because a small system with just a few discrete channels will be more prone to instability than a large system with an almost

continuous distribution of flow channels. If such effects persist at large enough scales, they may be significant in the transport of gas slowly generated in situ.

Our interpretation of pressure cycling as resulting from repeated blocking and unblocking of gas flow paths is supported by visual observations in Experiment A. Because of inaccuracy in the fabrication of this cast, the region of greatest aperture was along one edge of the fracture, and first gas flow was through this single path. When gas pressure rose at the inlet, and decreased at the outlet, a dead-end pore near the inlet was seen to expand like a surge chamber, and then collapse when the flow path became unblocked.[6] In Experiment B, Figure 3 shows that POC events along the lower flow path coincided with unblocking of a gas flow path (not necessarily the same flow path).

We now examine some examples of cycling pressures from Experiment C data, as shown in Figure 2. Regular pressure cycling, such as from 590.7 to 590.9 hours, suggests that blocking and unblocking are occurring at the same critical pore, while irregular cycling, such as during the period 590.5 to 590.7 hours, suggests that blocking and unblocking are occurring at several locations at different frequencies. Brief periods of time when no blocking occurred, such as from 531 to 533 and 536 to 537 hours, suggest that the phase occupancy was metastable and delicately balanced. Such periods only occurred twice during a month-long experiment, and only during the quietest time of night, suggesting that ambient vibrations caused the phases to lose their delicate balance.

As the gas:liquid flow rate ratio increases, it becomes easier for the gas flow to keep the gas flow path continuously open. The gas flow path is wider at its narrowest point, and less liquid is available to flow to the critical pore to block the gas flow. This occurred at condition 9 in experiment C, with k_{rg} = 14%, and condition 4 in experiment D, with k_{rg} = 12%.

RELATIVE PERMEABILITY

Relative permeability calculated from flow rate and pressure data are presented in Figures 5 and 6 for Experiments C and D, respectively. Calculation of permeability is discussed elsewhere.[6] Essentially, for a fracture the transmissivity, rather than the permeability, is calculated; the result is normalized to the liquid

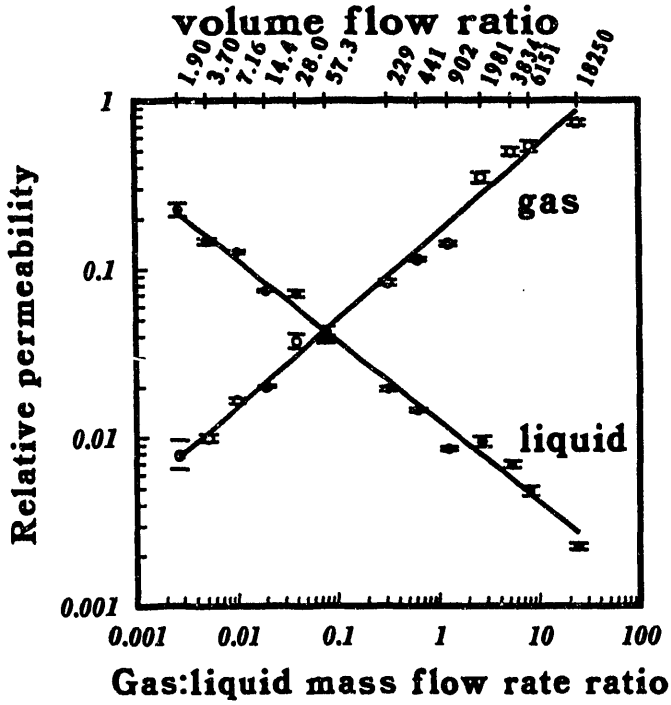

Figure 5. Relative permeability curves calculated from data of Experiment C, Stripa natural fracture.

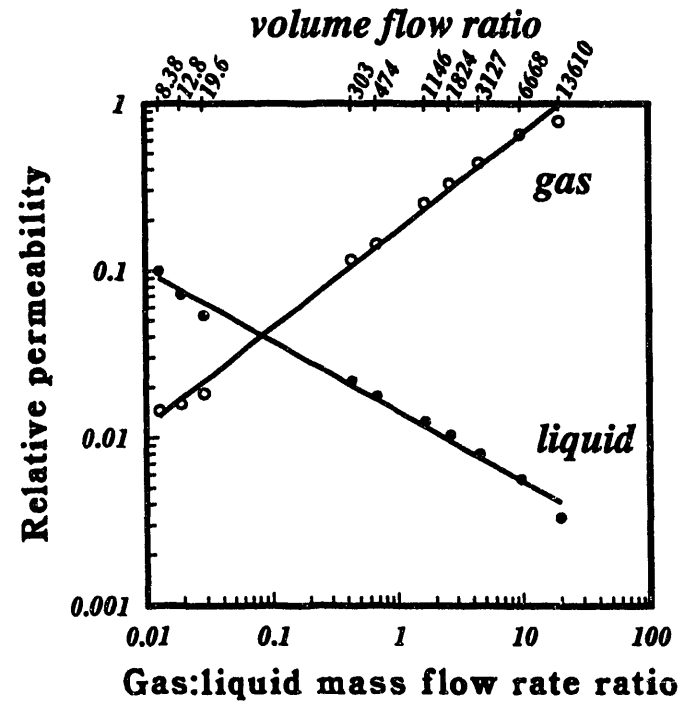

Figure 6. Relative permeability curves calculated from data of Experiment D, Dixie Valley fracture replica.

Table 3. Flow rates, pressures, and permeabilities in experiment D

Q_L (ml/hr)	ΔP_L (psi)	k_{rL}	Q_g (cm^3/min)	$P_{g\,IN}$ (psi)	$P_{g\,OUT}$ (psi)	k_{rg}	$P_{c\,IN}$ (psi)	$P_{c\,OUT}$ (psi)
0.90	7.21	0.0997	0.15[a]	21.57	14.40	0.0146	0.31	0.35
0.60	6.69	0.0717	0.15[a]	21.04	14.40	0.0160	0.30	0.36
0.40	5.94	0.0538	0.15[a]	20.24	14.33	0.0184	0.33	0.39
0.15	5.48	0.0218	0.85[b]	19.79	14.35	0.116	0.36	0.43
0.12	5.38	0.0176	0.77[b]	19.77	14.33	0.144	0.39	0.39
0.09	5.60	0.0125	1.37[b]	19.99	14.33	0.251	0.39	0.46
0.075	5.53	0.0104	1.80[b]	19.98	14.40	0.323	0.44	0.46
0.06	5.57	0.00804	2.40[b]	19.99	14.40	0.438	0.45	0.51
0.045	5.52	0.00566	3.55[b]	19.91	14.33	0.653	0.49	0.51
0.03	5.51	0.00332	4.25[b]	19.92	14.33	0.782	0.53	0.55

[a] measured at inlet gas pressure
[b] measured at one atmosphere pressure

transmissivity measured during single phase flow. Because saturation was not measured, flow rate ratio is plotted as the independent variable (in Experiment D, saturation could be calculated, in principle, by comparing the aperture map with observations of phase occupancy). Although the two fractures were quite different in geometry, the relationships of relative permeability to flow rate ratio are surprisingly similar; in both cases the relative permeability curves cross at approximately the same point, at flow ratio = 0.1 and relative permeability = 0.05. More work is needed, however, studying different fractures, fluids, and experimental conditions, before this behavior can be considered "typical" for fractures. In Experiment C, gas and liquid were always flowing, so no data are available for conditions in which only one phase is mobile. By contrast, in Experiment D, as gas invaded the fracture, although its own relative permeability was still zero, it occupied sufficient "pore space" to reduce the liquid permeability by about half.

The degree of phase interference is shown by plotting the gas and liquid permeabilities against each other, in Figure 7 Also shown for comparison are a curve for $k_{r,w} + k_{r,nw} = 1$ and a representative curve for porous media, calculated using the relationships of Corey[11] with typical values of 0.3 and 0.05 for irreducible saturations of liquid and gas respectively. The data for fractures show generally more severe phase interference than for porous media, with the sum of relative permeabilities being generally between 0.01 and 0.1.

In the second part of Experiment D, the outlet pressures of gas and liquid were controlled, and the inlet pressure of gas and the

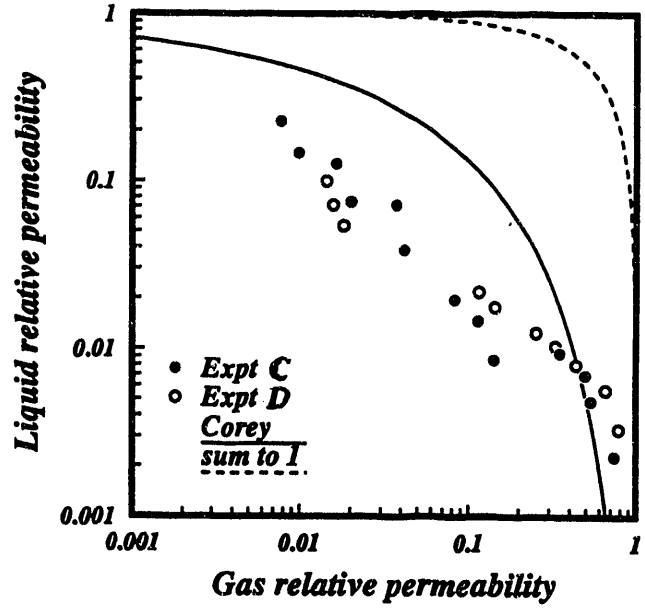

Figure 7. Relative permeabilities to gas and liquid, plotted against each other.

flow rate of liquid were controlled. With these constraints, the liquid inlet pressure is determined by the liquid relative permeability, and the inlet capillary pressure is the difference between the liquid inlet pressure and the gas inlet pressure. When the liquid flow rate was reduced stepwise, as shown in Table 3, the liquid inlet pressure decreased and the inlet capillary pressure increased as shown, and the outlet capillary pressure was adjusted to match it. In Figure 8, we plot relative permeability against inlet capillary pressure. This form of data is more useful for input to multiphase flow simulator models.

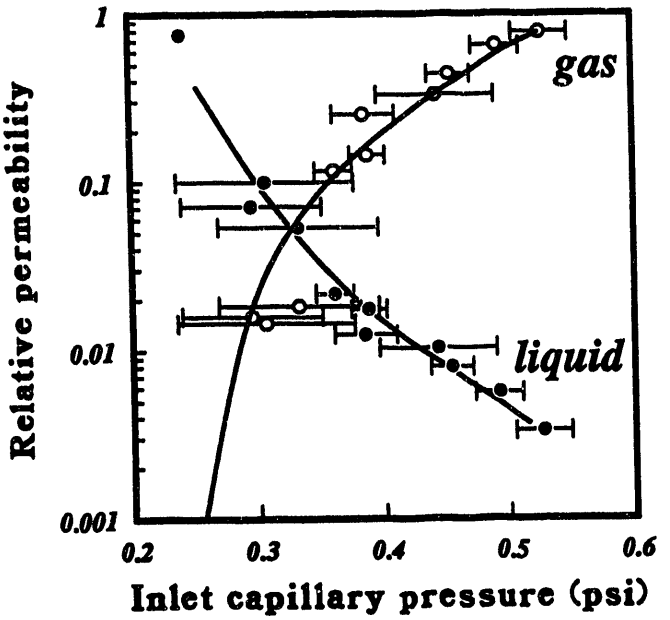

Figure 8. Relative permeability curves, plotted against capillary pressure, data of Experiment D.

SUMMARY

Two-phase flow of water and gas was visualized and measured in a natural rock fracture and transparent replicas under carefully controlled and monitored rate and pressure conditions. It was found that:

(1) Steady-state flow conditions are not easily achieved. Even when great care is taken to apply constant boundary conditions at the fracture, the two-phase flow behavior tends to persistent instabilities and phase occupancy changes.

(2) Phase interference is strong, as evidenced by the observation that both liquid and gas relative permeabilities are much less than 1 at intermediate saturations. This contrasts with the conventional view of fracture relative permeabilities that has held that the sum of two-phase relative permeabilities is near 1 at all saturations. However, our findings are in agreement with recent theoretical results for fractures conceptualized as two-dimensional porous media.

The laboratory work is ongoing. Attempts will be made to probe two-phase fracture flow on a larger scale, and for a broad variety of fractures and flow conditions (e.g., with non-horizontal fractures).

REFERENCES

1. K. PRUESS "Numerical Modeling of Gas Migration at a Proposed Repository for Low and Intermediate Level Nuclear Wastes at Oberbauenstock, Switzerland" LBL-25413, Lawrence Berkeley Laboratory (1977).

2. K. PRUESS and Y.W. TSANG, "On Two-Phase Relative Permeability and Capillary Pressure of Rough-Walled Rock Fractures," Water Resources Research, 26 (9), 1915-1926 (1990).

3. E.S. ROMM, Fluid Flow in Fractured Rocks (in Russian), Nedra Publishing House, Moscow (1966). (English Translation, W.R. Blake, Bartlesville, OK, 1972).

4. M.A. GRANT, "Permeability Reduction Factors at Wairakei," presented at AIChE-ASME Heat Transfer Conference, Salt Lake City, Utah (1977).

5. K. KARASAKI, S. SEGAN, and K. PRUESS, "Two-Phase Flow in Fracture Networks," Annual Report 1992, Earth Sciences Division, LBL-33000, Lawrence Berkeley Laboratory (1993).

6. P. PERSOFF, K. PRUESS, and L. MYER, "Two-Phase Flow Visualization and Relative Permeability Measurements in Transparent Replicas of Rough-Walled Rock Fractures," Proceedings, Sixteenth Workshop on Geothermal Reservoir Engineering, Stanford Univ., Stanford, CA., Jan. 23-25, 1991.

7. P. PERSOFF, K. PRUESS, and L. MYER, "Method and Apparatus for Determining Two-Phase Flow in Rock Fracture," U.S. Patent Application no. 07/909,937 July 7, 1992.

8. W.L. POWER and T.E. TULLIS, "The Contact Between Opposing Fault Surfaces at Dixie Valley, Nevada, and Implications for Fault Mechanics," Jour. Geophys. Research – Solid Earth, 97, 15425-15435 (1992).

9. B.L. COX and J.S.Y. WANG "Single Fracture Aperture Patterns: Characterization by Slit Island Analysis". This volume, (1993).

10. G.L. HASSLER, "Method and Apparatus for Permeability Measurements," U.S. Patent 2,345,935 (1944).

11. A.T. COREY, "The interrelationship between Gas and Oil Relative Permeabilities," Producers Monthly, 19, 38-41 (1954).

DATE
FILMED
7/21/93
END